Deformable Registration Using Regularization that Accommodates Local Tissue Rigidity

1. SUMMARY

Deformable medical image registration aims at retrieving the transformation $\boldsymbol{T}$ that brings the homologous image g's coordinate space into alignment into that of the reference image f, such that $f \approx g \circ \boldsymbol{T}$.

Deformable registration problems are most interesting due to its high flexibility but they are at the same time highly under-determined due to the extremely high dimensionality of transformation field, and this results in ill-conditioning as well as instability of solutions and local optima issues. Regularizations are introduced to alleviate these issues and also to incorporate prior physiological and anatomic knowledge into the problem formulation. Therefore, regularized deformable registration algorithms are usually set up to use a cost function, consisting of a similarity measure and a penalty term that discourages undesirable transformations. Conventional registration methods use homogeneous regularization for smoothness or other topological properties.

However, ignoring the elasticity difference between tissue types can result in non-physiological results, such as bone warping. Existing work addressing this issue either treats different regions of an image independently or post-filtering.

We propose a method to account for tissue-type dependent rigidity information by regularization design in nonrigid registration problem. Experiments with clinical data justifies that the proposed regularization design yields more physiologically sound deformation. As a additive penalty, it acts as a *"soft"* correcting force in high intensity regions, which tend to correspond to rigid structures towards locally rigid transformations, and relaxes within low intensity regions that tends to correspond to more elastic tissue types.

By designing the local stiffness factor as an implicit function via composition with an intensity map, our approach avoids explicit segmentation and is especially robust to partial volume effect, which is important when a multi-resolution technique is to be applied.

Moreover, the design of local rigidity penalty is based on the Frobenius norm, and each term involved in evaluating this function and its derivative (which is used in optimization step) is easily available from previous computation of the data fidelity metric. Therefore, the proposed approach hardly incurs any extra computation requirement.

2. OPTIMIZATION PROBLEM FORMULATION AND REGULARIZATION DESIGN

The goal of nonrigid registration is to find the transformation $\boldsymbol{T}^*$ such that the transformed homologous image g best matches the reference image f. We use Ω to denote the physical region of interest for registration. Let $\boldsymbol{T} : \Omega \to \Omega$ be the transformation. Let $\underline{x} \in \Omega$ denote the coordinate (in vector form) of a specific location. Our goal is to find:

$$\begin{aligned} \boldsymbol{T}^* &= \arg\min_{\boldsymbol{T}\in\Gamma} \Phi(\boldsymbol{T}, f, g) \\ &= \arg\min_{\boldsymbol{T}\in\Gamma} \{C(f, g \circ \boldsymbol{T}) + R(\boldsymbol{T})\}, \end{aligned} \tag{1}$$

where Γ is the class of allowable transformations. Here, the overall objective function Φ consists of two parts: data dis-similarity metric $C(f, g \circ \boldsymbol{T})$ and the regularization term $R(\boldsymbol{T})$ to penalize undesirable transformations.

2.1. L_2 norm for data (in)fidelity measure

Interested in deformable registration of helical and cone-beam CT images in particular, we use sum of squared difference (L_2 norm) to measure data infidelity *i.e.*,

$$C(f, g \circ \boldsymbol{T}) = \sum_{\underline{x}\in\Omega} (f(\underline{x}) - g(\boldsymbol{T}(\underline{x})))^2.$$

Note that the regularization design method applies generally to other data similarity metrics such as mutual information or correlation based metric.

2.2. Regularization Design

The regularization $R(\boldsymbol{T})$ is composed of two parts: a homogeneous spatial roughness penalty for deformation field, and a spatial varying (inhomogeneous) penalty that accounts for local tissue rigidity. The homogeneous smoothness penalty is defined as $\|\nabla \boldsymbol{D}\|_{Frob}^2$ and we design local tissue rigidity based penalty as $\sum_{\underline{x}} \gamma(\underline{x}) r(\boldsymbol{T}_{\underline{x}})$. The overall regularization becomes:

$$R(\boldsymbol{T}) = \gamma_s \|\nabla \boldsymbol{D}\|_{Frob}^2 + \sum_{\underline{x} \in \Omega} \gamma(\underline{x}) r(\boldsymbol{T}_{\underline{x}}).$$

where $r(\boldsymbol{T}_{\underline{x}})$ measures the deviation of the local transformation from being rigid, and $\gamma(\underline{x})$ is a spatial varying weight that reflects local tissue rigidity properties. In particular, $\gamma(\underline{x})$ can be looked on as the *local* "trade-off" between intensity match and tissue rigidity condition. It should be large where bone structure lies and small within more elastic regions. We also call it "*local stiffness factor*" to illustrate its physical meaning.

2.2.1. Non-Rigidity Index for Local Deformation

We design nonrigidity index for local deformation based on the following claims:

CLAIM 2.1. *A necessary and sufficient condition for a map $\boldsymbol{T}$ to be rigid at $\underline{x}$ is that its Jacobian matrix $\boldsymbol{J}_{\boldsymbol{T}}(\underline{x}) = \nabla \boldsymbol{T}(\underline{x})$ be orthogonal.*

LEMMA 2.2. *A necessary and sufficient condition for a matrix $\boldsymbol{M} \in \mathbb{R}^{d \times d}$ to be orthogonal is that $\left\|\boldsymbol{M}\boldsymbol{M}^T - \boldsymbol{I}_d\right\| = 0$, where $\|\cdot\|$ denotes any matrix norm.*

We have thus found a mathematically rigorous way to describe the deviation of the local transformation $\boldsymbol{T}_{vx}$ from being rigid. For simplicity, we choose to use the squared Frobenius norm, and design the rigidity regularization function to be:

$$r(\boldsymbol{T}_{\underline{x}}) \triangleq \left\|\boldsymbol{J}(\boldsymbol{T}_{\underline{x}})\boldsymbol{J}(\boldsymbol{T}_{\underline{x}})^T - \boldsymbol{I}_d\right\|_{\text{Frob}}^2.$$

or equivalently,

2.2.2. Local Stiffness Factor

We design the spatial varying local stiffness factor $\gamma(\underline{x})$ to reflect difference in elasticity among tissue types, which determines the relative weighting between data infidelity and deviation from rigidity.

FACT 1. *In calibrated X-ray CT images, pixel intensity (CT number) is highly correlated with tissue type information, hence a good inference source for local rigidity.*

Therefore, we define the local stiffness factor implicitly as the composition of a monotone increasing function h and the image intensity map f:

$$\gamma(\underline{x}) = h(f(\underline{x})).$$

In particular, we use a scaled and shifted hyperbolic tangent function due to its simplicity, sharp rising edge for distinguishing different tissue types and desirable satuation behavior intra tissue type. We choose the location and shape parameters for the hyperbolic function such that the rigidity penalty becomes strong and more dominant when in the bony structure, while much relaxed within elastic tissues.

In Fig. 1, we illustrate the derived stiffness map from reference image on the rightmost column.

2.2.3. Optimization

We adopt the commonly used B-spline basis to parameterize the deformation field and solve the optimization problem with the multi-resolution scheme.

$$\beta(\underline{x} - \underline{i}) = \beta(\frac{x}{\Delta_x} - i)\beta(\frac{y}{\Delta_y} - j)\beta(\frac{z}{\Delta_z} - k),$$

where $\underline{i} = [i, j, k]^T$ denotes the B-spline knot location, $\Delta_x, \Delta_y, \Delta_z$ determines the scale of B-spline in each direction, $\underline{x} = [x, y, z]^T$, and $\boldsymbol{N}(\cdot)$ is determined by the support of the B-spline basis.

In each resolution level, we use conjugate gradient method to iteratively solve for the B-spline coefficients until convergence.

3. EXPERIMENT SETUP

We tested our approach with two thorax CT scans of the same patient: one at 80% of the vital capacity inhale breath hold (deep inhale breath hold, tidal breathing generally peaks at 40% also) and one at exhale. The scans are both of size $512 \times 512 \times 148$ with voxel size $0.2 \times 0.2 \times 0.5cm^3$. We use the deep inhale breath-hold thorax CT image as the reference and further crop it to size $259 \times 175 \times 107$ to reflect the region of interest. Fig. 1 shows typical data slices (different views) of the reference image, homologous image and the inferred stiffness map ($h \circ f$).

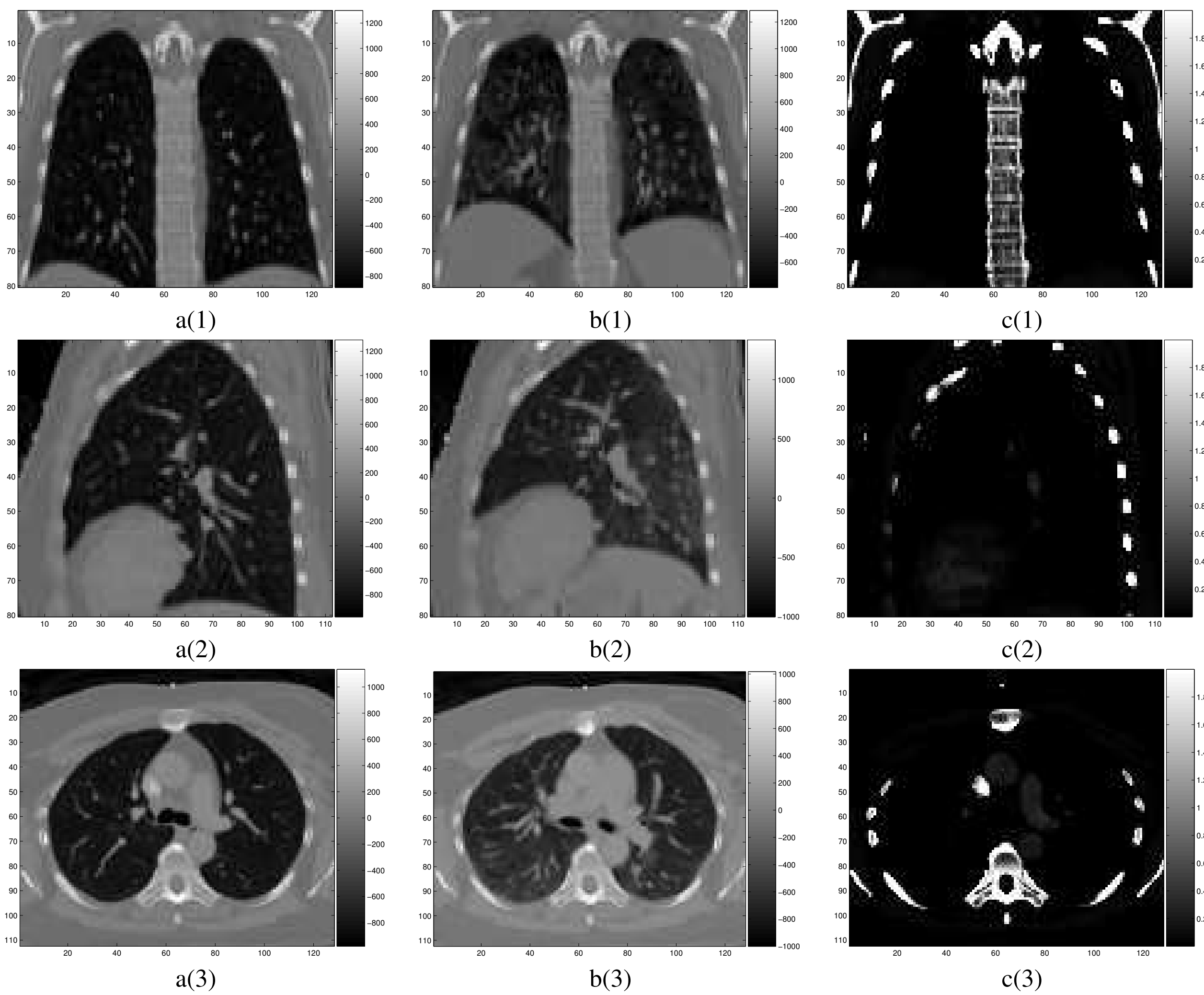

Figure 1. Different views of the original data and tissue information inferred from it. Top row [X(1)]: coronal slices; middle row [X(2)]: sagittal slices; bottom row [X(3)]: axial slices. Left column [a(#)]: slices from reference image; middle column [b(#)]: slices from homologous image; right column [c(#)]: slices from inferred stiffness map.

4. TEST RESULTS

We show the registration results in slice views by superimposing the deformed homologous image with reference image; and observe that including the proposed regularization term yields comparable intensity match as the the case with roughness penalty only in Fig. 2.

Notice that CT number is a very good indicator of tissue type, and bone structures corresponds to high count, we extract the bony structure by thresholding the CT number to check physiological soundness of the results. We overlay the

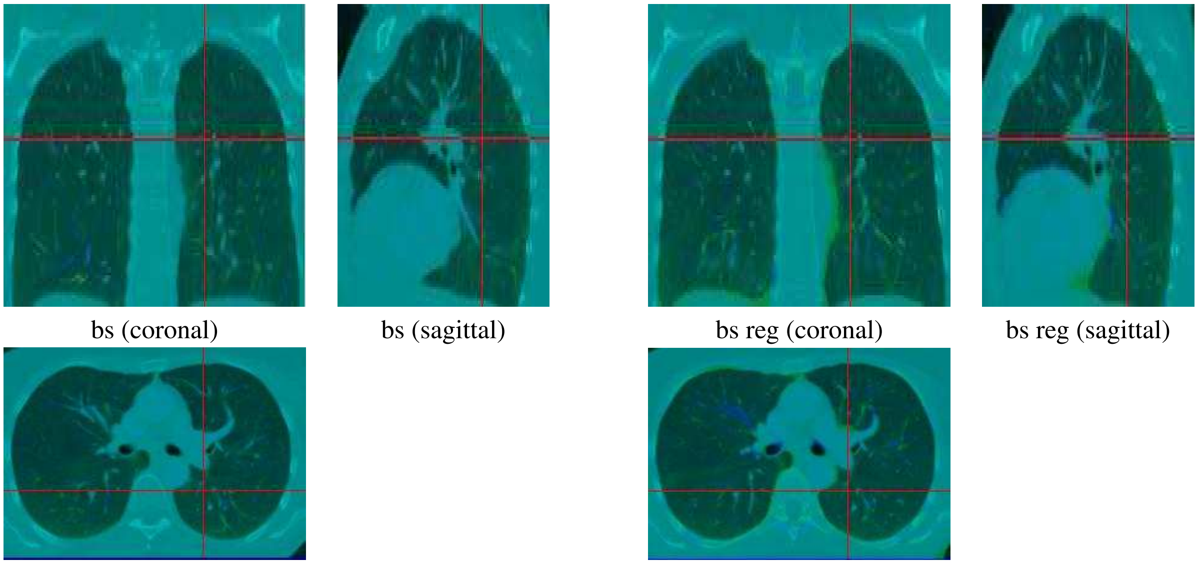

bs (coronal) bs (sagittal) bs reg (coronal) bs reg (sagittal)

bs(axial) bs reg (axial)

Figure 2. Deformed homologous image (green) overlaid with reference image (dark blue).: [bs(·)] B-Spline registration with smoothness penalty only; [bs reg(·)] B-Spline registration with both proposed regularization.

extract the geometry from the reference image volume (white) and the deformed homologous image (light blue) in Fig. 3to compare the performance in bone structure alignment.

We can clearly observe a nonphysical warping of bones in the deformed homologous geometry using B-spline based nonrigid registration method without the proposed regularization. This is due to the under-determinedness of B-Spline registration, *i.e.*, many local minima yield similar intensity matc. Inspecting closely where *"bone warping"* occur, we can see local minima of the data infidelity metric are mostly caused by the *"pseudo-periodic"* structure of the ribs. Moreover, the local smoothness property of B-Spline together with homogeneous smoothness regularization makes the bones to deform similarly as diaphragm where the motion is large, AKA, physical soundness is compromised to resemble elastic deformation in those regions.

When the proposed regularization is introduced, the deformation on the bone structures i given an additional *"force"* to conform to rigid transformation. We observe in Fig. 3 an obvious improvement as far as bone-warping issue is concerned.

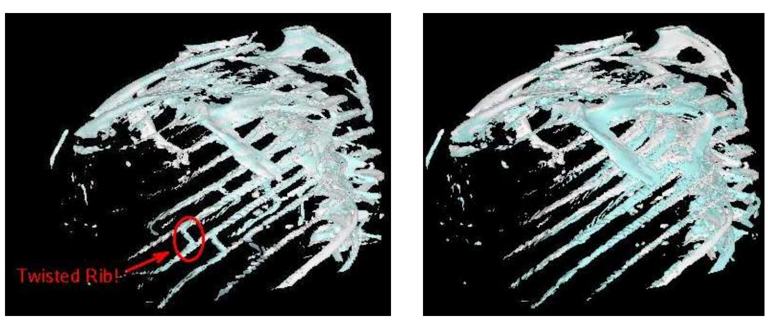

(a) (b)

Figure 3. Geometry extracted from registration results: (a) B-Spline based nonrigid registration with no local rigidity regularization; (b) B-Spline based nonrigid registration result with proposed local tissue type dependent regularization.